

## Characteristics and Optical Properties of Nano Ni Grains Reduced on TiO<sub>2</sub> Film

Hong-Hsin Huang<sup>1,\*</sup>, Hung-Peng Chang<sup>2</sup>, Fang-Hsing Wang<sup>2</sup>, Yuan-Shing Liu<sup>1</sup>,  
Moo-Chin Wang<sup>3</sup>, Ding-Fwu Lii<sup>1</sup>

<sup>1</sup>Department of Electrical Engineering, Cheng Shiu University,

840, Cheng Ching Rd., Niasong, Kaohsiung 83347, Taiwan

<sup>2</sup>Department of Electrical Engineering and Graduate Institute of Optoelectronic

Engineering, National Chung Hsing University,

250, Kuo Kuang Rd., Taichung 402, Taiwan

<sup>3</sup>Faculty of Fragrance and Cosmetics, Kaohsiung Medical University,

100, Shi-Chuan 1st Rd., Kaohsiung 80708, Taiwan

### Abstract

The NiO/TiO<sub>2</sub> films with various NiO film thicknesses ranging from 10 to 320 nm were deposited on silicon and glass substrates by E-beam evaporation at 200 °C, and then annealed in H<sub>2</sub> atmosphere at 500 °C for 1 h in order to reduce the NiO film to the Ni grains on TiO<sub>2</sub> film. The structures of titanium oxide, NiO and Ni/TiO<sub>2</sub> were analyzed by X-ray diffraction, and the morphology of Ni/TiO<sub>2</sub> films was observed by scanning probe microscopy. The UV-VIS transmittance and VIS absorption of Ni/TiO<sub>2</sub> film were measured by UV-VIS spectrophotometers. Results showed that the amorphous titanium oxide was obtained as deposited at 200 °C, and the structure transfer to anatase phase after 500 °C annealing. As deposited, the crystalline NiO films were obtained whose XRD patterns similar to that of powder, however, the diffraction peaks of (111) and (200) of Ni was appeared after annealing in H<sub>2</sub>

atmosphere. The Ni nano grains, coarsened grains and films were obtained on TiO<sub>2</sub> films when the NiO film of thickness from 10 to 320 nm reduced in H<sub>2</sub> atmosphere at 500 °C. The transmittance of Ni/TiO<sub>2</sub> films decreased with increasing Ni particle size. Whatever, the VIS absorption measurement showed that the peak shifted toward shorter wavelength with the decrease of Ni particle size.

**Keywords:** Nano Ni particle, Visible light absorption shift, Transmittance, E-beam evaporation, Morphology

Corresponding author: TEL: +886-7-7310606 ext.3409, FAX: +886-7-7337390

E-Mail: [funs@mail.mse.ncku.edu.tw](mailto:funs@mail.mse.ncku.edu.tw)

## 1. Introduction

Titanium dioxide (TiO<sub>2</sub>) films have benefic physical and chemical properties, which is one of the most important materials in optical, electronic and chemical fields. It is used as an anti- and high-reflection coating, capacitor, solar cell, photo-catalytic,<sup>1,2)</sup> and hydrophilic materials. New trends in reducing the size of microelectronic devices have enforced the use of high permittivity oxides to fabricate MOSFET structures with thicker oxides.<sup>3)</sup> Titanium oxide, zirconium oxide, and hafnium oxides are of immediate interest due to their high permittivity factor and compatibility with silicon technology.<sup>4-6)</sup> TiO<sub>2</sub> is generally considered to be the best semiconductor photocatalyst available for photocatalysis (PC) at present. Of possible greater significance are the recent findings of Fujishima et al.,<sup>7,8)</sup> that some semiconductors also exhibit a photo-induced superhydrophilic effect (PSH), i.e. they are rendered more wettable by water after exposure to ultra-band gap irradiation and that this process is reversible, albeit slowly, in the dark.

Metal-support interactions can affect both catalyst activity and stability.<sup>9)</sup> The technique of metal-doped TiO<sub>2</sub> photocatalysts preparation, thermal treatment, doping limitations, as well as doped titania properties and photoactivity were reviewed.<sup>10)</sup> Anpo et al.<sup>11)</sup> reported that visible light absorption is found for Cr-TiO<sub>2</sub> films by ion implanting process and the order of the effectiveness in the red shift was found to be V>Cr>Mn>Fe>Ni ions. Such a shift allows the metal ion-implanted titanium oxide to use solar light more efficiently and efficiently, at up to 20-30 %. On the other case, the Cr ion doped catalyst showed no shift in absorption band but a new absorption shoulder at around 420 nm. The modified method of metal on TiO should affect the absorption of visible light.

The Ni/TiO catalyst was prepared by Yan et al.<sup>12)</sup> for partial oxidation of

methane reaction (POM) and it showed a high activity and a long term stability in the CO reforming reaction. Yan et al. reported that CH<sub>4</sub> is efficiently converted to CO and H<sub>2</sub> via an oxidation mechanism when Ni/TiO<sub>2</sub> is reduced, and pulse reaction studies provide evidence that the oxidation state of nickel controls the methane activation mechanism and the product distribution. Titania-supported nickel catalysts were more active in CO hydrogenations than silica- or alumina-supported catalysts.<sup>13)</sup> Two groups of catalyst have been used for methane activation to generate syngas: Ni-based catalysts<sup>14)</sup> and noble-based catalysts<sup>15)</sup>. The high-cost and limited availability of noble metals highlights the need to develop Ni-based catalysts, which can exhibit stability for extended periods.

Titanium oxide thin film has been fabricated by E-beam evaporation,<sup>16)</sup> reactive and rf sputtering,<sup>17,18)</sup> thermal CVD,<sup>19)</sup> and plasma enhanced CVD<sup>20)</sup> techniques. E-beam evaporation is a powerful technique to prepared thin films with higher deposition rate and controlled stoichiometry by adjusting the deposition parameters such as substrate temperature, oxygen pressure and evaporation rate, etc.<sup>21,22)</sup> In this study, NiO/TiO<sub>2</sub> films with various NiO film thicknesses were deposited by E-beam evaporation on glass and silicon substrates and then annealed at 500 °C in H<sub>2</sub> atmosphere for 1 h in order to obtained Ni nano grains with various size on the crystalline TiO<sub>2</sub> film. The structure, morphology, UV-VIS transmittance and visible light absorption were studied.

## **2. Experimental**

The target materials of TiO<sub>2</sub> powder (ADMAT MIDAS Inc., 99.99 %) and NiO powder (Alfa Aesar, 99 %) were formed and sintered at 1200 °C for 3 h. The substrates were cleaned by isopropyl alcohol (EPA) and deionized water (DI water),

and then dried by nitrogen gas blowing. The substrate was fastened in a curved holder with a working distance of 20 cm and spin speed of 40 rpm. The substrates were heated by lamps to 200 °C. A diffusion-pumped vacuum system with a base pressure of  $5 \times 10^{-6}$  Torr was used for deposition. The deposition rate was controlled by E-beam power and monitored by a thickness control system (CRTM-6000, ULVAC, Japan). The TiO<sub>2</sub> thin films with thickness of 500 nm were deposited on silicon and glass substrates by E-beam evaporation at 200 °C and NiO thin films with thicknesses ranging from 10 to 320 nm were deposited on the TiO<sub>2</sub> film under the same deposition parameters. And then the NiO films were annealed at 500 °C in H<sub>2</sub> atmosphere for 1 h under a heating rate of 10 degree/min.

The structure of NiO, TiO<sub>2</sub> or Ni/TiO<sub>2</sub> films was identified by X-ray diffraction (XRD) with Cu K $\alpha$  radiation and a Ni filter, operated at 30 kV, 30 mA, a scanning rate of 4 °/min and 2 $\theta$  of 20° - 80° (model D5000, SIMENS, German). The morphology of the Ni/TiO<sub>2</sub> films was observed and analyzed by scanning probe microscopy, SPM (HV300, Seiko, Japan). The optical transmittance and absorption of Ni nano particle/TiO<sub>2</sub> thin film and glass substrate was measured by UV-VIS spectrophotometers (Agilent 8453, HP, USA) at 190 - 1100 nm and (U3010, Hitachi, Japan) at 200-800 nm.

### **3. Results and Discussion**

Titanium oxide film was deposited on glass and silicon substrates by E-beam evaporation at 200 °C, whose structure was analyzed by XRD as shown in Fig. 1. It reveals that the amorphous titanium oxide was obtained either on silicon or glass substrates. For thin film deposition, amorphous titanium oxide is usually obtained at low deposition temperatures. The mobility of the absorbed species is relatively low

due to low substrate temperature, thus preventing these species from migrating to more energetic sites where nucleation can occur.<sup>23)</sup> Amor et al.<sup>24)</sup> reported that the amorphous titanium oxide film prepared by radio frequency magnetron sputtering was obtained at temperature lower than 350 °C although high energy ion bombardment was used in sputtering process, and the unheated films are amorphous whatever the sputtering parameters.<sup>25)</sup> The color of titanium oxide prepared at room temperature was transparent, but a little gray color was observed when deposited at 200 °C. Although the color of the thin film had changed, the structure of titanium oxide was still amorphous as shown in Fig. 1.

The NiO film was deposited on TiO<sub>2</sub>/silicon or TiO<sub>2</sub>/glass by E-beam evaporation and the structure was analyzed by XRD as shown in Fig. 2. In Fig. 2, the (111), (200), (220) and (311) reflections of NiO thin film was obtained and intensity ratio is close to the data of JCPDs card, which reveals that the polycrystalline NiO film with a random orientation was obtained. There was no preferred orientation was found, which was usually found in thin film deposition processes.

The NiO films deposited on TiO<sub>2</sub>/silicon or TiO<sub>2</sub>/glass by E-beam evaporation with various thicknesses and then annealed at 500 °C in H<sub>2</sub> atmosphere for 1 h. The structure of Ni/TiO<sub>2</sub> films analyzed by XRD was given in Fig. 3. Although titanium oxide exists three different phases: anatase, rutile and brookite, only amorphous, anatase and rutile films have been found in TiO<sub>2</sub> films up to now.<sup>26)</sup> The key factors influencing the microstructure of TiO<sub>2</sub> film are deposition temperature and annealing temperature.<sup>24,27)</sup> At low temperature, the TiO<sub>2</sub> film with anatase phase is more stable and transfers to rutile phase about 800 °C.<sup>24)</sup> In Fig. 3, it was found that the anatase TiO<sub>2</sub> film was obtained, meanwhile, the diffraction peaks are nearly maintained constant after annealed at 500 °C. The structure of the crystalline TiO<sub>2</sub> films are

anatase phase with reflections of (101), (112), (200) and (204) as shown in Fig. 3. Battiston et al.<sup>28)</sup> reported that a thermal treatment at 500 °C in air for 3 h is not sufficient to induce phase transformation to anatase and a transformation is observed only after 6 h of annealing in air at 500 °C. Such reluctance to crystallization is more marked in samples grown at low temperatures. In this study, the TiO<sub>2</sub> film was prepared by E-beam evaporation followed annealing at 500 °C for 1 h which shorter than Battiston et al. used. However the sharp diffraction peaks of anatase phase were found in Fig. 3. Application for photocatalyst, the anatase phase has the highest photocatalytic activity<sup>29)</sup> and is good choice for anticorrosion effect under UV illumination. Either of anatase and rutile phase is usually observed in the films prepared by PVD or CVD process. In Fig. 3, we can also find that the intensity of Ni diffraction peaks, i.e. (111), (200) and (220), increases as the thickness of NiO film increases, which indicates that the particle size of Ni increased with the thickness of NiO film increasing. Until the thickness of NiO film was higher than 80 nm, the Ni grains connected and began to form a thin film after annealing in H<sub>2</sub> atmosphere for 1 h. These samples with metallic color were observed and very low resistivity was easily measured.

After annealing, Ni nano grains were reduced from NiO film on TiO<sub>2</sub> film. The surface morphologies of Ni/TiO<sub>2</sub> films on silicon substrates were observed by SPM as shown in Fig. 4, and the influence of particle size has been studied. In Fig. 4(a), the isolated nano Ni grains formed, whose average size is less than 100 nm. It was found that the thicker NiO film thickness, the larger Ni particle. Furthermore, isolated grains coarsened and contacted each other resulting in island grain formation, and then a Ni film finally formed. In Fig. 4(c), a distinct morphology was found because of nickel film formation. From Fig. 4, it demonstrated that the nano Ni grains on TiO<sub>2</sub> film

could be prepared by NiO film reduction and the average particle size of Ni could be decided by NiO film thickness.

Titanium oxide films are transparent in visible region and its transparency exhibits a sharp decrease in the UV region.<sup>30)</sup> The transmittance of Ni-TiO<sub>2</sub> films was shown in Fig. 5 which shows that the transparent limitations are nearly at constant because the TiO<sub>2</sub> films deposited in same run were annealed at the same temperature of 500 °C. Martin et al.<sup>31)</sup> reported the similar results when TiO<sub>2</sub> films were annealed lower than 700 °C, but the limitation shifted to higher wavelength after annealing at 900 °C and 1100 °C. Hou et al.<sup>32)</sup> reported that the transparent limitation would shift to longer wavelength because of rutile/anatase ratio of the films after various temperature annealing. It can be observed that the shape of the spectra depends not only on the changes in the nickel layer thickness, but also on the changes of particle size. The transmittance decreased with the increase of Ni particle size, and very low transmittance was found when Ni film formed. In Fig. 5, the similar peak shape was found, but these peaks shift to shorter wavelength with the increase of Ni nano particle size. At the same time, the transmittance decreased with the increase of nano Ni particle size, because the transparent area was occupied by Ni grains. Yoon et al.<sup>33)</sup> reported that the visible light absorption wavelength move forward the shorter wavelength because of the size of nano-metallic particle decreased. According to our previous research, the highest transparent ratio of TiO<sub>2</sub> film on glass is higher than 90%, however, the lower transparent ratio was found because of Ni nano grains.

The VIS absorption of Ni/TiO<sub>2</sub> films was showed in Fig. 6 which reveals that the effect of Ni nano particle/TiO<sub>2</sub> film on the visible light absorption is obvious. We will find the absorption peak shifts to longer with Ni grain size increasing.



#### **4. Conclusion**

The nano Ni grains reduced on TiO<sub>2</sub> film could be prepared by way of NiO/TiO<sub>2</sub> films deposited by E-beam evaporation followed annealing in H<sub>2</sub> atmosphere at 500 °C for 1 h. The Ni particle size increases with the increase of NiO film thickness, and grains coarsened and finally connected to form a thin film when NiO film thickness is higher than 80 nm. For transmittance measurement, the peak shift to shorter wavelength and the trend increased with the decrease of Ni particle size. For visible light absorption measurement, the absorption peak shifted toward longer wavelength with the increase of Ni particle size.

#### **Acknowledgements**

Financial support from the Nation Science Council, Taiwan, ROC through a grant No. NSC93-2216-E-2310-006 is greatly appreciated. The authors also sincerely thank Dr. S.J. Huang and Dr. C.H. Tai for their kind assistance in transmittance measurements.

## Reference

1. M. Takahashi, K. Mita and H. Toyuki: *J. Mater. Sci.* 24 (1989) 243.
2. K. Ishibashi, Y. Nosaka, K. Hashimoto and A. Fujishima: *J. Phys. Chem.* B102 (1998) 50.
3. C. Hobbs, R. Hegde and B. Maiti: *Symposium on VLSI Technology Digest of Technical Papers, 1999*, pp. 133J–135J.
4. P.S. Peercy: *Nature* 406 (2000) 1023.
5. A.I. Kingon, J.-P. Maria and S.K. Streiffer: *Nature* 406 (2000) 1032.
6. H. Sim, S. Jeon and H. Hwang: *Jpn. J. Appl. Phys.* 40 (2001) 6803.
7. A. Fujishima, R. Wang, K. Hashimoto, T. Watanabe, M. Chikuni, E. Kojima, A. Kitamura and M. Shimohigoshi: *Adv. Mater.* 10 (1998) 135.
8. A. Fujishima, T.N. Rao and D. Tryk: *J. Photochem. Photobiol. C: Photochem. Rev.* 1 (2000) 1.
9. M.C.J. Bradford and M.A. Vannice: *Appl. Catal. A* 142 (1996) 73.
10. M.I. Litter: *Appl. Catal. B: Environ.* 23 (1999) 89.
11. M. Anpo, M. Takeuchi, K. Ikeue and S. Dohshi: *Current Opinion in Solid State and Materials Science* 6 (2002) 381.
12. Q.G. Yan, W.Z. Weng, H.L. Wan, H. Toghiani, R.K. Toghiani and C.U. Pittman, Jr: *Applied Catalysis A* 239 (2003) 43.
13. M.A. Vannice and R.L. Garten: *J. Catal.* 56 (1979) 236.

14. D. Dissanayake, M.P. Rosynek, K.C.C. Kharas and J.H. Lunsford: *J. Catal.* 132 (1991) 117.
15. C.T. Au and H.Y. Wang: *J. Catal.* 167 (1997) 337.
16. L.-J. Meng, M. Andritschky and M.P. dos Santos: *Thin Solid Films* 223 (1993) 242.
17. M. Nakamura, T. Aoki and Y. Hatanaka: *Vacuum* 59 (2000) 506.
18. M. Ivanda, S. Music, S. Popovic and M. Gotic: *J. Mol. Struct.* 480-481 (1999) 645.
19. D.H. Lee, Y.S. Cho, T.S. Kim, J.K. Lee and H.J. Jung: *Appl. Phys. Lett.* 66 (1995) 815.
20. Y.H. Lee, K.K. Chan and M.J. Brady: *J. Vac. Sci. Technol. A* 13 (1995) 596.
21. K. Kawasaki, J.F. Despres, S. Kamei, M. Ishikawa and O. Odawara: *J. Mater. Chem.* 7 (1997) 2117.
22. F. Zhang, X. Liu, Y. Mao, N. Huang, Y. Chen, Z. Zheng, Z. Zhou, A. Chen and Z. Jiang: *Surf. Coat. Technol.* 103–104 (1998) 146.
23. X. Hou and K.-L. Choy: *Surf. Coat. Tech.* 180–181 (2004) 15–19
24. S.B. Amor, L. Guedri, G. Baud, M. Jacquet and M. Ghedira: *Mat. Chem. Phys.* 77 (2002) 903.
25. S.B. Amor, G. Baud, M. Jacquet and N. Pichon: *Surf. Coat. Tech.* 102 (1998) 63.

26. P. Löbl, M. Huppertz and D. Mergel: Thin Solid Films 251 (1994)72.
27. Y.-Q. Hou, D.-M. Zhuang, G. Zhang, M. Zhao and M.-S. Wu: Appl. Surf. Sci. 218 (2003) 97.
28. G.A. Battistona, U.R. Gerbasia, A. Gregoria, M. Porchiaa, S. Cattarinb and G.A. Rizzic: Thin Solid Films 371 (2000) 126.
29. B. Ohtani, Y. Ogawa and S.I. Nishimoto: J. Phys. Chem. B 101 (1997) 3746.
30. D. Mardare, M. Tasca, M. Delibas and G.I. Rusu: Appl. Surf. Sci. 156 (2000) 200.
31. N. Martin, C. Rousselot, D. Rondot, F. Palmينو and R. Mercier: Thin Solid Films 300 (1997) 113.
32. X. Hou and K.-L. Choy: Surf. Coat. Tech. 180 –181 (2004) 15.
33. J.W. Yoon, T. Sasaki and N. Koshizaki: Electrochem. Solid-State Lett. 5 (2002) A256.

### **Figure captions**

Fig. 1 XRD pattern of titanium oxide film deposited on silicon substrate at 200 °C.

Fig. 2 XRD pattern of nickel oxide film deposited on titanium oxide at 200 °C.

Fig. 3 XRD patterns of Ni/TiO<sub>2</sub> film reduced from NiO/TiO<sub>2</sub> films with thicknesses of (a) 10, (b) 20, (c) 40 (d) 80 (e) 160 nm NiO film.

Fig. 4 SPM analysis of Ni/TiO<sub>2</sub> film reduced from NiO/TiO<sub>2</sub> films with thicknesses of (a) 10, (b) 40, (c) 160 nm NiO film.

Fig. 5 UV-VIS transmittance of Ni/TiO<sub>2</sub> film reduced from NiO/TiO<sub>2</sub> films with thicknesses of (a) 10, (b) 20, (c) 40 (d) 80 (e) 160 nm NiO film.

Fig. 6 VIS absorption of Ni/TiO<sub>2</sub> film reduced from NiO/TiO<sub>2</sub> films with thicknesses of (a) 10, (b) 20, (c) 40 (d) 80 (e) 160 nm NiO film.

Fig. 1, 7.5 cm in width

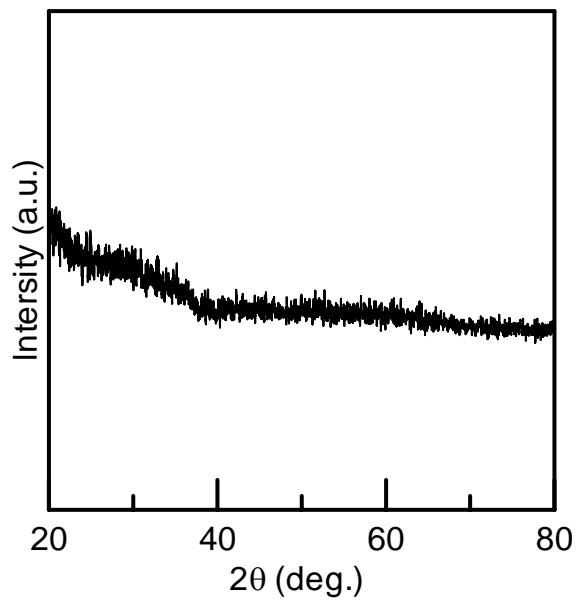


Fig. 2, 7.5 cm in width

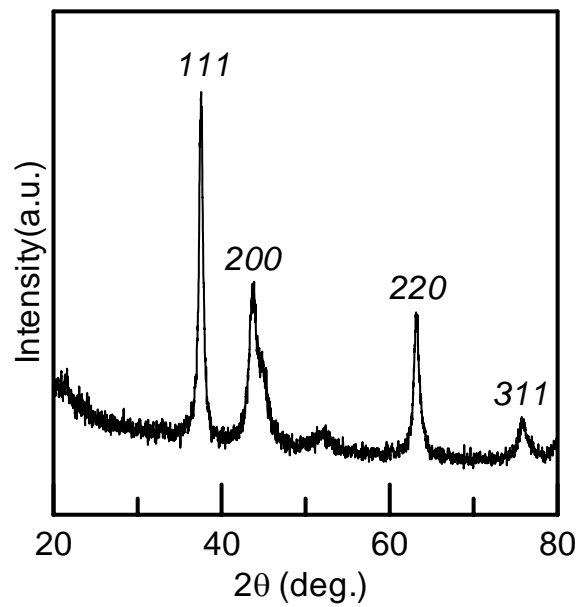


Fig. 3, 7.5 cm in width

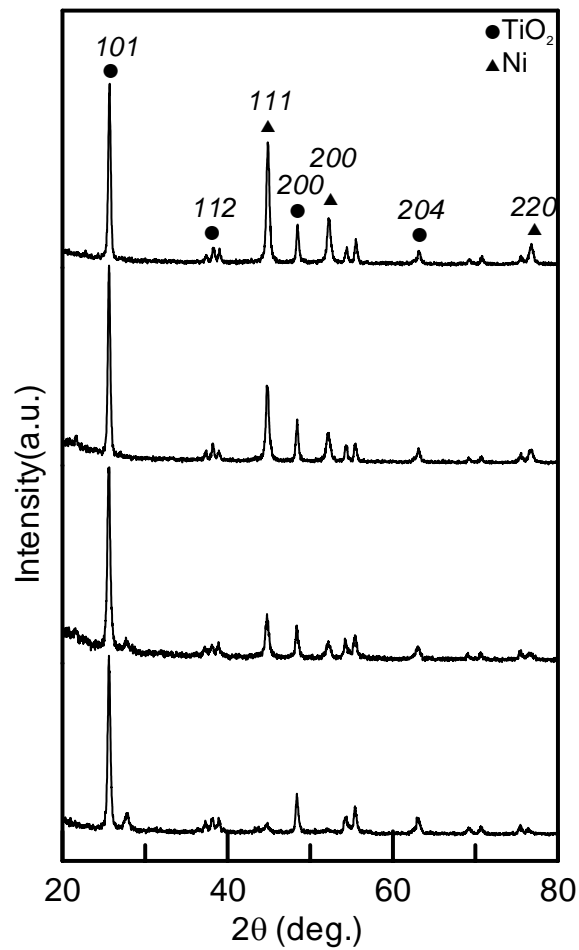




Fig. 4, 7.5 cm in width

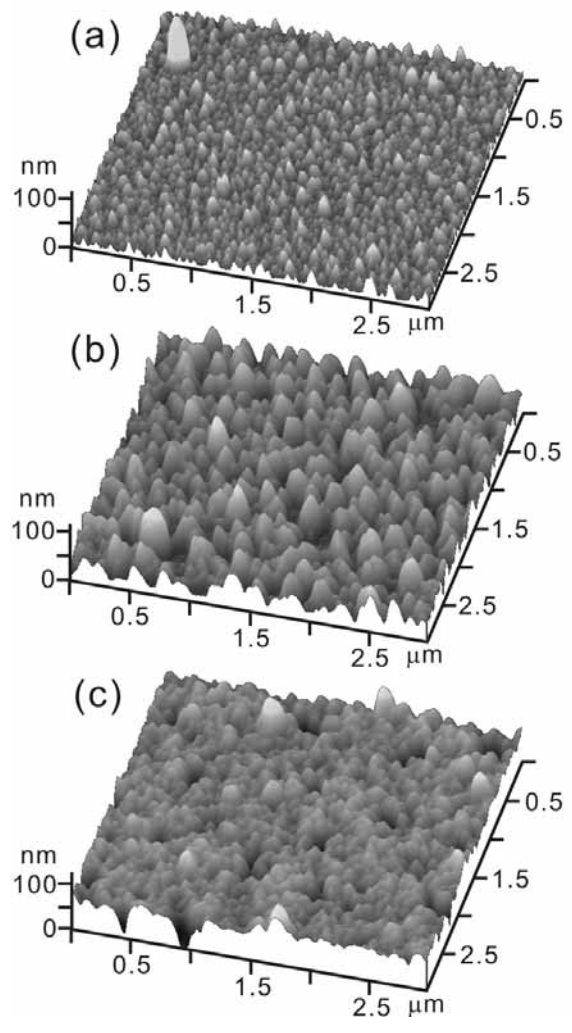


Fig. 5, 7.5 cm in width

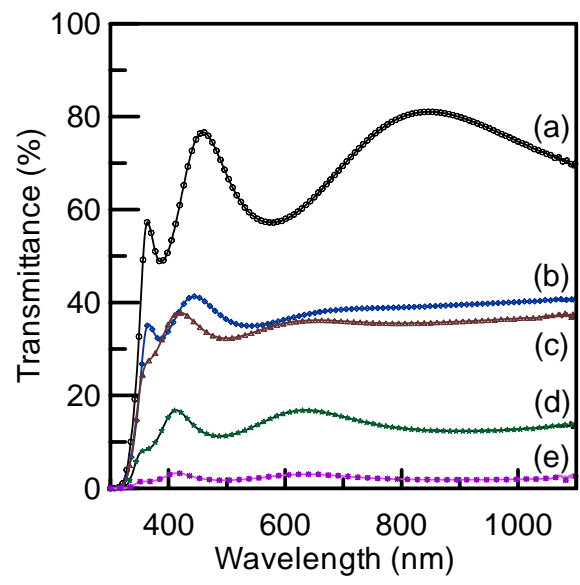


Fig. 6, 7.5 cm in width

